

# SCALING LAWS FOR NORMAL CONDUCTING $e^+e^-$ LINEAR COLLIDERS

J.-P. Delahaye, G. Guignard, I. Wilson/CERN, T. Raubenheimer /SLAC.

## Abstract

Design studies of a future TeV  $e^+e^-$  Linear Collider (TLC) are presently being made by five major laboratories within the framework of a world-wide collaboration. A figure of merit is defined which enables an objective comparison of these different designs. This figure of merit is shown to depend only on a small number of parameters. General scaling laws for the main beam parameters and linac parameters are derived and prove to be very effective when used as guidelines to optimize the linear collider design. By adopting appropriate parameters for beam stability, the figure of merit becomes nearly independent of accelerating gradient and RF frequency of the accelerating structures. In spite of the strong dependence of the wakefields with frequency, the single bunch emittance preservation during acceleration along the linac is also shown to be independent of the RF frequency when using equivalent trajectory correction schemes. In this situation, beam acceleration using high-frequency structures becomes very favourable because it enables high accelerating fields to be obtained, which reduces the overall length and consequently the total cost of the linac.

## 1 INTRODUCTION

A lot of progress has been made in the last ten years on design and development studies towards high-luminosity TeV-range Linear Colliders (TLC). Various options for efficient beam acceleration have been explored and periodically compared within the framework of a world-wide collaboration [1]. Two basic technologies have been developed for beam acceleration: TESLA proposes to use 1.3 GHz super-conducting (SC) structures whereas SBLC, JLCc, JLCx, NLC, VLEPP and CLIC have chosen normal-conducting travelling-wave (NCTW) structures operating at the very different frequencies of 3, 5.6, 11.4, 14 and 30 GHz, respectively. General scaling laws have been derived [2] for multi-bunch TLCs which use NCTW structures, taking into account the basic physics processes which have been used to optimise the different designs. For completeness, the graphs also include data points for both TESLA and VLEPP in spite of their respective SC and single bunch operation. The motivation for the scaling study is two-fold. First, by comparing the parameters adopted by the various design studies which cover a decade in operating frequency, the study provides an insight into the way the different optimisations have been achieved. Secondly, it provides a logical strategy based on objective, physics-based arguments for designing or re-optimising any new or presently-proposed linear collider.

## 2 LUMINOSITY - FIGURE OF MERIT

The luminosity of an  $e^+e^-$  linear collider is given by:

$$L = \frac{k_b N_b^2 f_{rep}}{4\pi \bar{\sigma}_x^* \bar{\sigma}_y^*} = \frac{N_b P_b}{4\pi e U_f \bar{\sigma}_x^* \bar{\sigma}_y^*} = \frac{H_D N_b \eta_{RF}^{AC} \eta_b^{RF} P_{AC}}{4\pi e U_f \bar{\sigma}_x^* \bar{\sigma}_y^*} \quad (1)$$

where  $P_{AC}$ ,  $\eta_{RF}^{AC}$  and  $\eta_b^{RF}$  are the AC power, the AC-to-RF and RF-to-beam efficiencies,  $U_f$ ,  $P_b$ , and  $N_b$  are the beam energy, beam power and number of particles per bunch,  $\bar{\sigma}_x^*$  and  $\bar{\sigma}_y^*$  are the r.m.s. beam sizes at the Interaction Point (I.P.) after being pinched by the beam-beam interaction, and  $H_D$  is the corresponding luminosity enhancement factor. Each particle is decelerated by the beam-beam interaction losing on average an energy  $\delta_b$  and emitting  $n_\gamma$   $\gamma$ -rays. At c.m. energies  $< 2$  TeV the parameters are chosen such that  $\delta_b$  does not exceed a few %, this is the so-called low beamstrahlung (LB) regime. At higher energies, to get adequate luminosity, the parameters are chosen in the high beamstrahlung (HB) regime [3]. In the HB regime, where  $n_\gamma = 3.5\delta_b$ , choosing  $n_\gamma \approx 2$  ensures a reasonable compromise between the fraction of total luminosity contributed by particles with energies within 1-2 % of the maximum, and the number of  $e^\pm$  pairs which appear as background in the detector. In both regimes therefore  $\delta_b$  is an essential design parameter. The assumption of flat beams ( $\sigma_x \gg \sigma_y$ ) to enhance the luminosity and to decrease  $\delta_b$  leads to the following expressions in the LB and HB regimes:

$$\delta_B \propto \frac{U_f N_b^2}{\sigma_z \bar{\sigma}_x^{*2}} \quad \text{and} \quad \delta_B \cong \frac{n_\gamma}{3.5} \propto \frac{\sigma_z^{1/3} N_b^{2/3}}{U_f^{1/3} \bar{\sigma}_x^{*2/3}} \quad (2)$$

Using (1), (2), and assuming in the LB regime a vertical beta function at the I.P. equal to the bunch length to minimise the ‘‘hourglass’’ effect, the luminosity scales as:

$$L \propto \frac{\delta_B^{1/2} H_{Dy} \eta_{RF}^{AC} \eta_b^{RF} P_{AC}}{U_f \epsilon_{ny}^{*1/2}} \quad \text{and} \quad L \propto \frac{\delta_B^{3/2} H_{Dy} \eta_{RF}^{AC} \eta_b^{RF} P_{AC}}{U_f^{1/2} \beta_y^{*1/2} \sigma_z^{1/2} \epsilon_{ny}^{*1/2}} \quad (3)$$

In both cases, the luminosity only depends on a small number of parameters. For objective comparisons, a figure of merit  $M$ , is defined as  $L$  normalised to  $P_{AC}$ ,  $\delta_B$ , and  $U_f$ . Neglecting the variations of  $H_D$  (small for a flat beam) and of  $\eta_{RF}^{AC}$  (similar in all designs),  $M$  becomes:

$$M = L \frac{U_f}{\delta_B^{1/2} P_{AC}} \propto \frac{\eta_b^{RF}}{\epsilon_{ny}^{*1/2}} \quad \text{and} \quad M = L \frac{U_f^{1/2}}{\delta_B^{3/2} P_{AC}} \propto \frac{\eta_b^{RF}}{\sigma_z^{1/2} \epsilon_{ny}^{*1/2}} \quad (4)$$

*The TLC design optimisation consists of selecting beam parameters, and choosing a technology that is able to accelerate, at a reasonable cost, a high power beam with an optimum AC-power to beam-power conversion efficiency (Sections 3 and 4) while preserving a very small vertical normalised beam emittance (Section 5).*

### 3 RF POWER TO BEAM EFFICIENCY

The RF-to-beam conversion efficiency is directly related to the choice of the RF frequency and the beam parameters. In order to obtain a high RF-to-beam transfer efficiency, all TLC designs (except VLEPP) have chosen to operate with a large number of bunches. In the extreme case of an infinite number of bunches, the formulation of the RF to beam efficiency becomes extremely simple [2] with a dependency on only two parameters: the field attenuation constant of the structures,  $\tau$ , and the normalised beam current,  $J$ :

$$\eta_b^{RF} = \frac{2\tau g(\tau) J}{\left[1 + \frac{J}{2} \left(1 - \frac{e^{-2\tau}}{g(\tau)}\right)\right]^2} \quad (5)$$

$$\text{where } J = \frac{R' q_b}{G_a \Delta_b} = \frac{R' I_b}{G_a} \quad (6)$$

and  $R'$ ,  $I_b$ ,  $q_b$ ,  $\Delta_b$ ,  $G_a$ ,  $G_a$  are respectively the shunt impedance per meter, the beam current, the charge per bunch, the interval between bunches, the unloaded and loaded accelerating gradient. For a given  $J$ , there is a value  $\tau_{opt}$  which maximises the RF to beam efficiency:

$$\tau_{opt} = \frac{G_u \Delta_b}{R' q_b} = \frac{1}{J(1-\delta)} \quad (7)$$

Using accelerating structures with an optimum field attenuation,  $\tau_{opt}$ , following equation (7), and for the more usual range of beam parameters,  $0.5 \leq J \leq 2$ , where the beam loading parameter  $\delta$  is limited to 50% (Fig. 1), the scaling of  $\eta_b^{RF}$  and  $\tau_{opt}$  is approximated by:

$$\eta_b^{RF} \propto (J)^{1/2} = \left(\frac{R' q_b}{G_a \Delta_b}\right)^{1/2} \quad \text{and} \quad \tau_{opt} \propto J^{-9/10} \quad (8)$$

Here,  $\propto$  is the approximate proportionality implied by the straight line fit in Fig. 1 over the range of parameters considered. The figure of merit then becomes:

$$M \propto \frac{\eta_b^{RF}}{\varepsilon_{ny}^{*1/2}} \propto \left(\frac{J}{\varepsilon_{ny}^*}\right)^{1/2} = \left(\frac{R' q_b}{\varepsilon_{ny}^* G_a \Delta_b}\right)^{1/2} \quad (9)$$

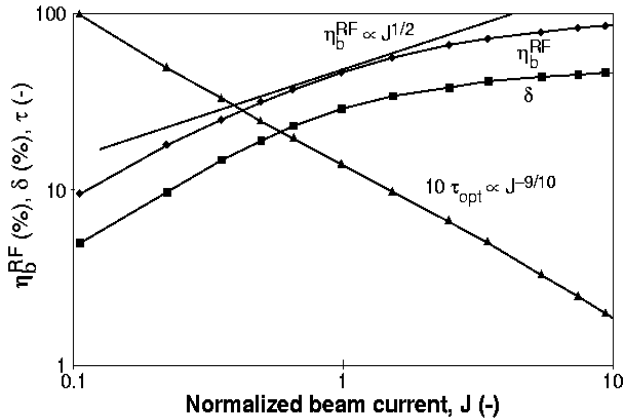


Figure 1: Optimum RF to beam efficiency,  $\eta_b^{RF}$ , field attenuation,  $\tau$ , and beam loading parameter,  $\delta$ .

### 4 THE NORMALIZED BEAM CURRENT

To optimise the design of a linear collider, the beam and linac parameters are therefore chosen to maximise the  $J$  parameter while preserving the initial vertical normalised beam emittance. All four parameters in the expression for  $J$ , (eq. 6) are directly related to the RF frequency,  $\omega$ , of the accelerating structures. This is why the different TLC designs are mostly frequency driven.

• The well known scaling with frequency of  $R'$ , when taking into account the iris to wave-length ratio,  $a/\lambda$ , is well verified in the TLC designs (Fig.2):

$$R' = r' Q \propto \omega^{1/2} (a/\lambda)^{-1} \quad (10)$$

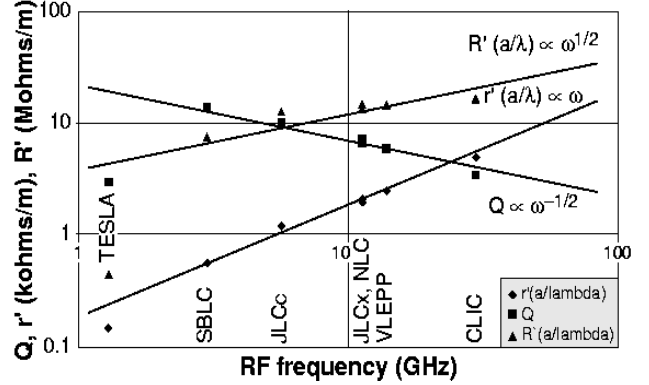


Figure 2: Accelerating structure parameters.

• The minimum distance between bunches is limited by the transverse wakefield level that can be obtained at the second and subsequent bunches by damping and/or detuning. For a given type of structure the number of RF periods needed for the same relative wakefield reduction is constant. This is reflected in Fig. 3 which shows that in spite of the different structure designs, the distance between bunches adopted in the various TLC designs scales with the RF wavelength:

$$\Delta_b \propto \omega^{-1} \quad (11)$$

The  $J$  parameter then becomes:

$$J = \frac{R' q_b}{G_a \Delta_b} \propto \omega^{3/2} (a/\lambda)^{-1} G_a^{-1} N_b \quad (12)$$

The charge per bunch is therefore made as high as possible to maximise  $J$ . Its maximum value is limited by beam stability considerations as developed in section 5.

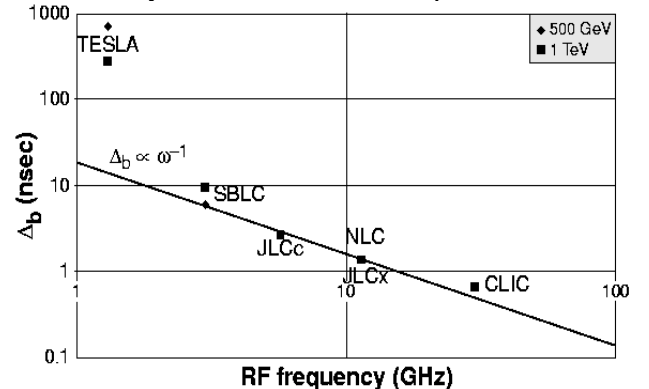


Figure 3: Time interval between bunches.

## 5 BEAM EMITTANCE PRESERVATION

Very small vertical normalised beam emittances of a few  $10^{-8}$  rad-m are expected from state-of-the-art damping rings presently under development. During acceleration along the several-kilometer-long linacs however, the beams suffer a transverse blow-up  $\Delta\varepsilon_n$ , which is especially important in the vertical plane because of the particularly small initial emittance. One of the primary causes of emittance blow-up comes from the transverse wake-fields induced by the misalignment of the accelerating structures and by the beam trajectory deviations.

### 5.1 BNS damping

The single-bunch beam stability is greatly improved by so-called BNS damping [4] using a correlated energy spread which is introduced along the bunch such that:

$$\Delta p / p = \delta_{BNS} \propto N_b \langle W_T \rangle \frac{\langle \beta \rangle \langle L_{CELL} \rangle}{U} \quad (13)$$

where  $\langle \beta \rangle$  is the mean betatron amplitude of the focusing optics along the linac, and  $W_T$  is the short range transverse wakefield averaged over the bunch with an r.m.s. length,  $\sigma_z$ , and scaling as:

$$\langle W_T \rangle \propto W_T' \sigma_z \propto \omega^4 (a/\lambda)^{-7/2} \sigma_z \quad (14)$$

Under BNS damping conditions when taking into account equation (14), the vertical blow-up induced by the transverse wake-fields [5] shows a strong dependence (to the eighth power) on the frequency:

$$\langle \Delta\varepsilon_{ny} \rangle_{RF} \propto N_b^2 \sigma_z^2 (a/\lambda)^{-7} \omega^8 G_a^{-1} \langle \beta_0 \rangle L_s \langle \Delta y_{RF}^2 \rangle \quad (15)$$

but the other parameters in equation (15) also scale strongly with the frequency as shown hereafter.

### 5.2 Bunch length

The bunch length,  $\sigma_z$ , is made as small as possible in order to decrease the average transverse wakefield in the bunch according to equation (14). However, the minimum acceptable bunch length is determined by the need to compensate, towards the end of the linac, the energy spread associated with the longitudinal wake-fields, by positioning the bunch off the crest of the accelerating RF wave. Thus:

$$\frac{N_b W_L}{G_a} \propto \sigma_z \omega \sin(\Phi_{RF}) \Rightarrow \sigma_z \propto N_b G_a^{-1} (a/\lambda)^{-2} \omega \quad (16)$$

where  $W_L$  is the short range longitudinal wakefield and  $\Phi_{RF}$  is the off-crest RF phase which is limited to small values for the sake of beam acceleration efficiency.

### 5.3 Ratio of iris radius to RF wavelength

As shown in Fig. 4 for the different TLC designs, the ratio of iris radius to RF wavelength,  $a/\lambda$ , increases with increasing frequency in order to minimise the effect of the transverse wakefields (equation 14):

$$a/\lambda \propto \omega^{1/5} \quad (17)$$

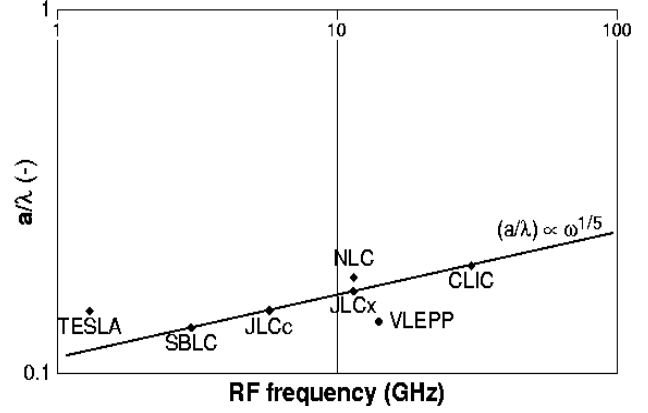


Figure 4: Iris to wavelength ratio.

### 5.4 Focusing optics of the linacs

In order to limit the BNS momentum spread needed for beam stability (eq. 13), the focusing strength along the linac is usually increased with the operating frequency as shown in Fig. 5. This is possible at higher frequencies because of the reduction in size of the linac components. Assuming the inner diameter,  $D$ , of the quadrupoles is scaled inversely with frequency in the same way as the inner radius of the iris,  $a$ , of the RF structures, then for the same magnetic field on the poles,  $B$ , the same phase advance per cell,  $\beta_p$ , and the same quadrupole filling factor,  $F$ , the FODO cell length,  $L_{cell}$ , scales as follows:

$$L_{cell} \propto \frac{D}{FL_{cell}B} \Rightarrow \langle \beta_0 \rangle \propto L_{ocell} \propto (a/\lambda)^{1/2} \omega^{-1/2}$$

### 5.5 Pre-Alignment tolerances of the RF structures

Since the size of the accelerating structures becomes smaller with increasing frequency, the accuracy with which they can be made and pre-aligned is expected to approximately scale with the inverse of the frequency. As seen in Fig. 6, the variation of the pre-alignment tolerances of the RF structures in all TLC designs is well approximated by the following scaling law with frequency, which indeed is very close to expectation:

$$\langle \Delta y_{RF} \rangle \propto \omega^{-3/4} \quad (19)$$

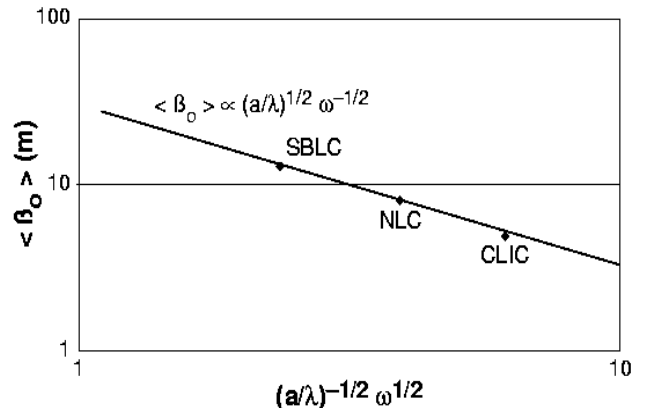


Figure 5: Focusing optics at injection into the linac.

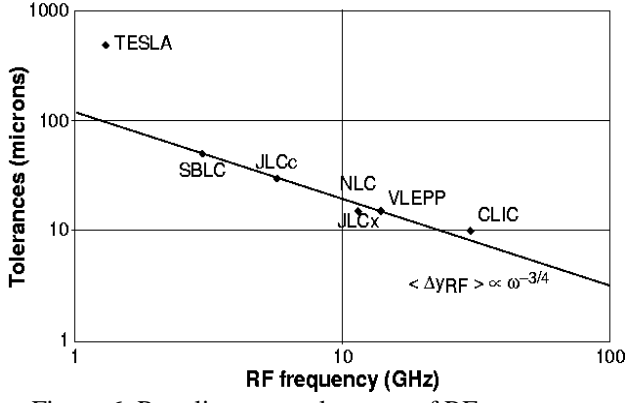


Figure 6: Pre-alignment tolerances of RF structures.

### 5.6 Accelerating section length

The length of the accelerating section,  $L_s$ , is adjusted to obtain an optimum field attenuation parameter,  $\tau_{opt}$ , to maximise the RF-to-beam efficiency (equation 7)

$$L_s = \frac{2Qv_g\tau_{opt}}{\omega} = \frac{2Qv_g}{\omega J(1-\delta)} \quad (20)$$

Neglecting the variation of the beam loading parameter  $\delta$ , for small  $\delta$  values, and introducing the scaling for  $J$  (eq. 6) as well as of the quality factor  $Q$  and the group velocity  $v_g$ , the optimum length of the accelerating sections, in the extreme case of an infinite number of bunches, becomes:

$$L_s \propto \omega^{-3} (a/\lambda)^4 G_a N_b^{-1} \quad (21)$$

### 5.7 Charge per bunch

Finally, it is possible to derive the scaling of the maximum charge per bunch. This is the charge which produces a tolerable and frequency-independent beam blow-up during acceleration. It is deduced by substituting the relations for the scaling of all the different parameters (eq. 16, 17, 18, 19 and 21) in eq. 15.

$$(\Delta \varepsilon_{ny})_{RF} \cong Const. \Rightarrow$$

$$N_b \propto \omega^{-5/3} (a/\lambda)^{13/6} G_a^{2/3} \propto \omega^{-6/5} G_a^{2/3} \quad (22)$$

After substitution of eq. 22 for  $N_b$  in eq. 13, 16, and 21,

$\sigma_z$ ,  $L_s$ , and  $\delta_{BNS}$  become:

$$\sigma_z \propto \omega^{-2/3} (a/\lambda)^{1/6} G_a^{-1/3} \propto \omega^{-2/3} G_a^{-1/3} \quad (23)$$

$$L_s = \frac{2Qv_g\tau_{opt}}{\omega} \propto \omega^{-4/3} (a/\lambda)^{11/6} G_a^{1/3} \propto \omega^{-1} G_a^{1/3} \quad (24)$$

$$\delta_{BNS} \propto \omega^{2/3} (a/\lambda)^{-1/6} G_a^{1/3} \propto \omega^{2/3} G_a^{1/3} \quad (25)$$

As shown in Figs 7, 8, 9 and 10, the charge per bunch, the bunch length, the length of the accelerating structure and the theoretical momentum spread for BNS damping adopted in the TLC designs compare favourably with the above scaling laws.

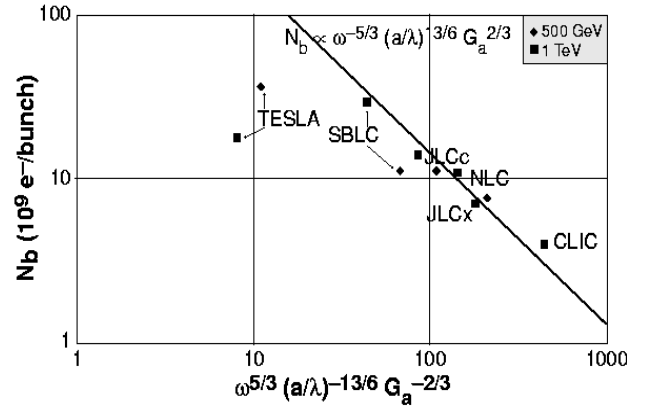


Figure 7: Charge per bunch.

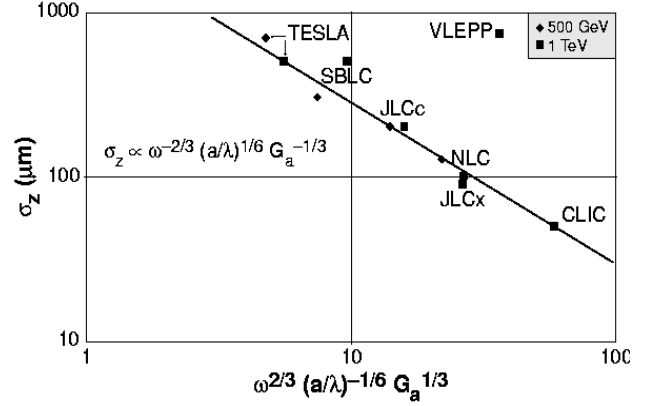


Figure 8: Bunch length.

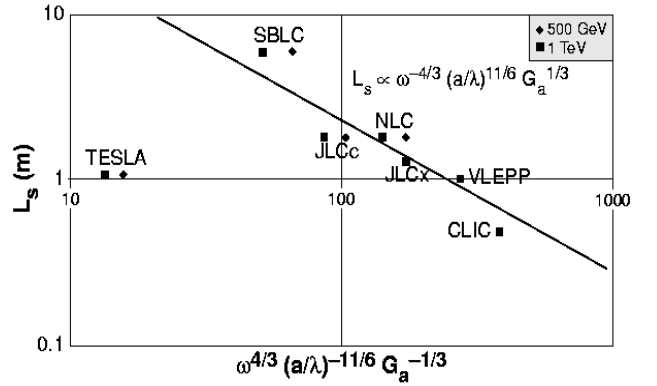


Figure 9: Length of the accelerating structures.

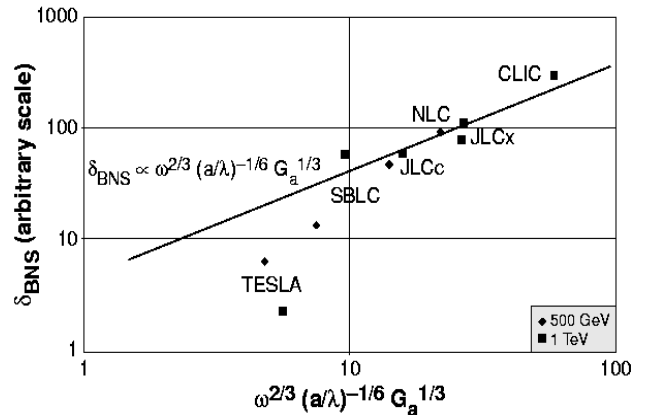


Figure 10: Momentum spread for BNS damping.

The strong dependence on frequency of the vertical blow-up induced by transverse wakefields is therefore cancelled by an appropriate choice of the other parameters and reduced to an acceptable level in all the TLC designs, independently of the RF frequency:

$$\varepsilon_{ny}^* \propto \varepsilon_{ny} = \varepsilon_{nyo} + \Delta\varepsilon_{ny} \quad \text{with} \quad \Delta\varepsilon_{ny} \cong \text{Const.} \quad (26)$$

There is also a contribution [5] to  $\Delta\varepsilon$  coming from the beam position monitor (BPM) misalignments. The same condition (26) on the emittance growth produces for  $\Delta y_{BPM}$  the generally expected dependence with  $\omega^{-1}$  (Section 5.5),

$$\langle \Delta y_{BPM} \rangle \propto \omega^{-1/4} G_a^{1/6} \langle \Delta y_{RF} \rangle \propto \omega^{-1} G_a^{1/6} \quad (27)$$

Finally, by introducing the frequency laws obtained up to this point, the normalised beam current and the RF-to-beam efficiency become roughly independent of the RF frequency and accelerating gradient,

$$\eta_b^{RF} \propto J^{1/2} \propto \omega^{-1/12} (a/\lambda)^{7/12} G_a^{-1/6} \propto \omega^{1/30} G_a^{-1/6} \quad (28)$$

## 6 SENSITIVITY TO GROUND MOTION

The slow ground motion, modelled by the standard ATL law [6], causes all linac components to move with time. If uncorrected, the resulting trajectory variation will lead to emittance dilution [7]. The dominant effect comes from the quadrupoles with a contribution

$$\Delta\varepsilon_{nQUAD} \propto ATN_{cell}^3 \delta_{BNS}^2 \quad (29)$$

where  $N_{cell}$  is the number of focusing cells in the linac, which is proportional to  $L_{cell}$  and  $G_a$ . Thus, using the above scaling laws, the time interval required between corrections to limit the emittance growth is

$$T_{QUAD} \propto \frac{G_a^{7/3} \varepsilon_{ny}}{A\omega^{5/2}} \left( \frac{\Delta\varepsilon_{ny}}{\varepsilon_{ny}} \right)_{ATL} \quad (30)$$

The equivalent time interval related to cavity drift shows a similar dependence  $\propto G_a^{1/3} \omega^{-5/3}$ . Finally, the high frequency vibration of the focusing magnets induces a pulse-to-pulse trajectory variation which cannot be corrected with beam-based feedbacks. In local beam-size units, this induced beam jitter is [5]:

$$\frac{\langle \Delta y^2 \rangle}{\sigma_y^2} \approx \langle y_{QUAD}^2 \rangle \frac{4U_0 N_{CELL}}{\varepsilon_{ny} L_{oCELL}} \left( \frac{U_f}{U_o} \right)^{(1-\alpha)} \tan\left(\frac{\Psi}{2}\right) \quad (31)$$

where  $y_{QUAD}$  is the focusing magnet movement. As a consequence, the vibration tolerance scales as:

$$\langle y_{QUAD}^2 \rangle \propto \frac{\langle \Delta y^2 \rangle}{\sigma_y^2} \frac{G_a}{\omega^{2/3}} \varepsilon_{ny} \quad (32)$$

## 7 CONCLUSION

The figure of merit  $M$ , defined in Section 2, has been used to optimise the design of a future TeV  $e^+e^-$  Linear Collider.  **$M$  is only dependent on two parameters: the AC-to-beam power transfer efficiency and the vertical beam emittance at the IP.** Scaling laws have been

derived for both the linac and beam parameters for an infinite number of bunches, stable beam operation and minimum energy spread at the linac end. Under these conditions, the main beam parameters are fully determined. Using them, and choosing an optimum field attenuation for the RF structures in order to obtain an optimum RF-to-beam efficiency, it is found that:

- **The RF-to-beam efficiency is a weak function of the frequency and accelerating gradient** (Eq.28)
- In spite of the large increase of the wake-field amplitude with frequency, **the wakefield effect and the corresponding beam emittance blow-up are independent of the RF frequency** (Eq. 26), **for equivalent beam trajectory correction techniques.**
- **In the low-beamstrahlung regime**, generally adopted for intermediate-energy TLC designs (0.5 to 2 TeV), **the luminosity slightly increases with RF frequency and slightly decreases with accelerating gradient**

$$L \propto \frac{\delta_B^{1/2} \eta_{RF}^{AC}}{U_f} \frac{\omega^{1/30} G_a^{-1/6}}{\varepsilon_{nyo}^{1/3} [1 + \Delta\varepsilon_{ny} / \varepsilon_{nyo}]^{1/2}} P_{AC}$$

- **In the high-beamstrahlung regime**, usually adopted for high-energy TLC designs (3 to 5 TeV), **the luminosity increases with RF frequency but is independent of accelerating gradient**

$$L \propto \frac{\delta_B^{3/2}}{U_f^{1/2}} \frac{\eta_{RF}^{AC}}{\beta_y^{*1/2}} \frac{\omega^{1/3}}{\varepsilon_{nyo}^{1/2} [1 + \Delta\varepsilon_{ny} / \varepsilon_{nyo}]^{1/2}} P_{AC}$$

**Finally, the use of high frequencies in accelerating structures for main linacs of future TeV  $e^+e^-$  Linear Colliders is particularly appropriate, since they allow operation with high accelerating gradients, which minimise the overall length and therefore the cost of the linacs. Provided that the beam and linac parameters are chosen to fulfil beam stability criteria and optimum RF-to-beam transfer efficiency, high frequency designs benefiting from high accelerating gradients result, when compared to lower frequency designs with lower gradient and similar beam quality, with the same or better RF efficiency and figure of merit.**

## 8 REFERENCES

- [1] Int. Linear Collider Technical Review Committee Report, ed. G. Loew, SLAC-R-95-471, 1995.
- [2] J.P. Delahaye *and 3 co-authors*, CERN/PS/97-51, 1997 and CLIC Note 333.
- [3] J.P. Delahaye *and 6 co-authors*, Proc. PAC97, Vancouver, Canada, and CERN/PS 97-23, 1997.
- [4] V.E. Balakin, *and 3 co-authors*, Proc. 12<sup>th</sup> Int. Conf. On High Energy Accelerators, Fermilab, 1983.
- [5] T.O. Raubenheimer, CLIC Note 347, 1997.
- [6] B. Baklakhov, *and 5 co-authors*, INP 91-15; Tech. Ph.38, 984, 1993.
- [7] A. Sery and O. Napoly, Phys. Rev. E 53, 5323, 1996.